Pointing models for the 40 m radiotelescope at 6, 8 and 22 GHz

P. de Vicente

Informe Técnico IT-OAN 2010-11

Revision history

Version	Date	Author	Updates
1.0	07-04-2010	P. de Vicente	First version

Contents

1 Introduction

This report describes results from several pointing sessions at 6, 8 and 22 GHz. The whole pointing session spanned more than two months. The procedure, described below, was iterative at the three frequencies. All observations were performed using continuum detector OAY14 and an integration time of 1 second. The simultaneous bandwidth used was that of the frontend bandwidth: 500 MHz in the three cases. Data were analyzed with CLASS in continuum mode.

The 40 m antenna is a Nasmyth telescope with receivers in different locations. The beam is directed towards the requested receiver by removing or inserting mirrors in the signal path. Each of these Nasmyth mirrors introduce pointing errors and hence the pointing model should not necessarily be the same for all receivers. Barcia (see de Vicente & Barcia 2007) studied the influence of the misalignment of Nasmyth mirrors and horns on the pointing model of the telescope. Parameters P_1, P_2, P_5, P_7, P_8 and P_9 may contain terms due to misalignments of optical elements after mirror M2 (the subreflector).

As with technical report OAN-2010-10, the works regarding pointing were interrupted by the adjustement of the surface of the radiotelescope. Therefore this report is a summary of the status of the telescope by August 2010. Further works will be performed in the future since some issues regarding pointing are still open. These issues have been mentioned along this report and are related to the optimum position of the X band and 22 GHz horns.

2 Observing strategy

The aim of a pointing campaign is to obtain a good pointing model of the antenna, characterized in our case by a set of 8 parameters with a physical meaning. If these parameters are unknown or poorly determined they cause azimuth and elevation errors which depend on elevation and azimuth and are proportional to the errors in the parameters. See de Vicente & Barcia (2007) and de Vicente (2008a) for the algorithm used in the 40 m. Parameters are obtained by least square analysis and the fit improves when the coverage of azimuth and elevation is best.

Pointing campaigns are made of several sessions of pointing drifts on sources with different right ascention and declination. The trajectory of each source on the sky allows to sample part of the sky. In order to maximize the sky coverage it is important to choose 5 or 6 bright sources whose declinations produce different elevations when they transit the local meridian.

There are two strategies to observe several sources from their rise to their set: the simplest one is to track each source for a long time and then proceed with the next one. A better strategy is to perform one double pointing scan on each source and repeat the cycle. Some sources will be over the horizon, and others will be below at a given time. Therefore the cycle at any time is done with those sources which are visible. This solution minimizes the observing time, provides a good sky coverage and prevents systematic effects.

Results in this report were obtained using both strategies. We used the first observing mode at the beginning of the campaign. The second was used for more than half of the results presented here. Fig. 1 shows examples of the sky coverage for both strategies. To the left, the sources are tracked from rise to set and once a source is finished another source is tracked. To the right, the antenna makes a double pointing drift on one source and then moves to another

and this is repeated for 5 or 6 sources in total. This cycle is repeated for 24 hours and a good sky coverage is obtained after 1 day.

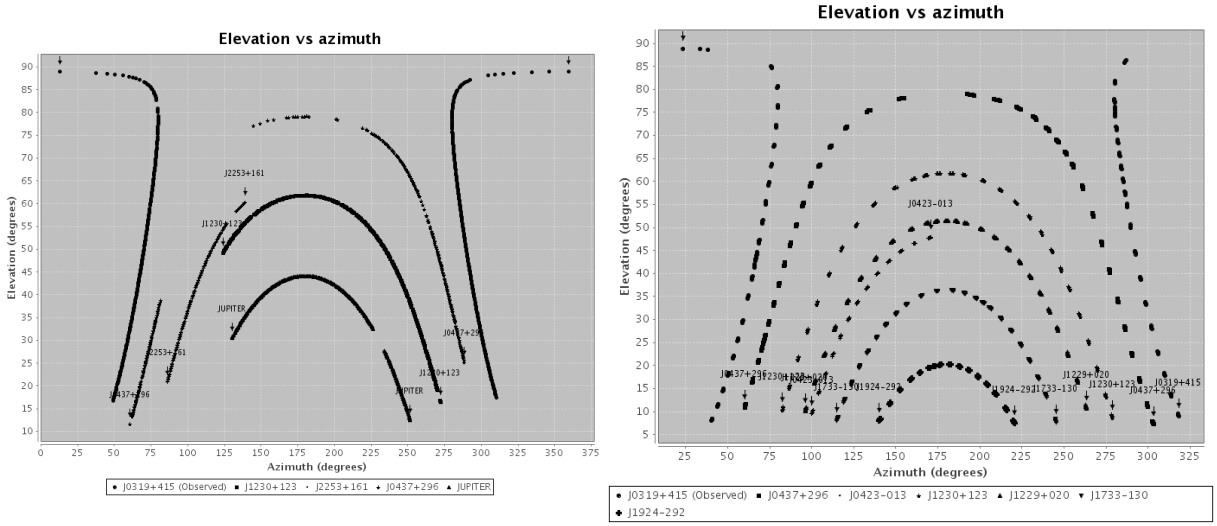

Figure 1: *Sky coverage using two different strategies. X axis is azimuth and Y axis elevation. Left: Sources were tracked continuously from rise to set. The coverage took 4 days. Right: Sources were tracked alternatively using a cycle. The coverage took 24 hours. The right one takes less time and avoids systematic errors. No circumpolar sources where observed*

3 Open issues: Histeresis and double drifts

The pointing model used in the 40 m telescope up to March 2010 was obtained by a manual fit, and it is described by de Vicente (2008b). This model has been used for 2 and a half years for all receivers since no solution for the elevation encoders problem (de Vicente et al 2010a) was found until 2010. After studying the problem and while we wait for further results and a definitive diagnostic and solution, elevation encoder 2 has been deactivated and is no longer used in the position loop of the antenna. Deactivation of encoder 2 reduces the hysteresis problem but does not solve it completely.

Figure 2 shows the measured errors at several elevations at 22 GHz using only encoder 1. Pointing drifts moving previously the antenna from the horizon and from the zenith were done on 3C84, DR21 and Jupiter. The difference of pointing errors obtained coming from zenith and from horizon (prior to making the pointing) versus elevation is depicted in that figure. Errors decrease at high and low elevations and are larger at mid elevations. The maximum error caused by hysteresis using only encoder 1 is $\simeq 14''$ and hence the pointing model accuracy is limited by this value. Real observations may show errors lower than the previous value because they depend on the previous position of the antenna.

Double pointing drifts show a systematic effect of unknown effect that we hope to fix in the future. The pointing error between a go and return drift is always half the space moved by the

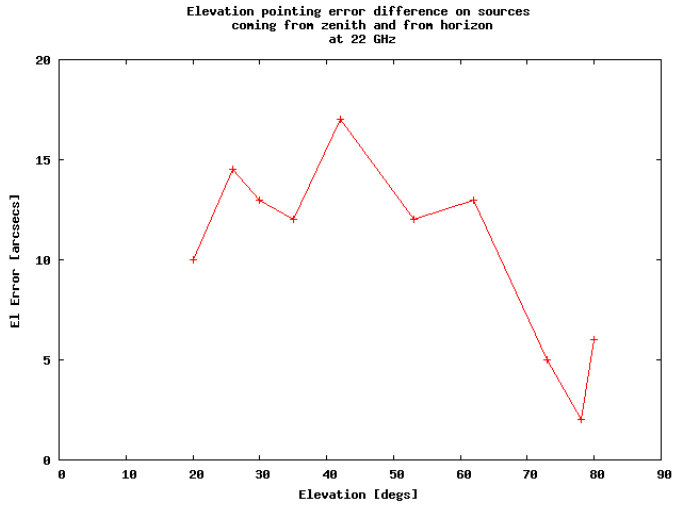

Figure 2: *Elevation pointing error difference between two pointing drifts on a source. On pointing drift was preceed by moving the driving from the zenith and the other by driving it coming from the horizon. Pointing errors are always higher when coming from the zenith. Encoder 2 was deactivated*

antenna in the integration time. It happens as if the source were always found 1/4 the integration interval after it is expected. Figure 3 shows that effect on azimuth and elevation drifts at 22 GHz, where the integration interval is $10''$. This effect should not have a relevant effect on the pointing model since the average is 0, but increases the data dispersion. The possible cause is a software bug which has not been identified yet.

4 The Nasmyth mirror effect

As stated in de Vicente & Barcia (2007), a receiver positioning error in a Nasmyth telescope causes modifications on pointing parameters P_1, P_3, P_8 and P_9. We will describe here the positioning error for a horn in a plane perpendicular to the direction of radiation after being reflected on a flat Nasmyth mirror (M3 in our case) and on a second mirror with magnification that we will call M5.

Let us assume a reference frame for a given horn, where X is an axis parallel to the ground and perpendicular to the direction of radiation and Y is an axis perpendicular to the ground and perpendicular to the direction of radiation, and that the horn is misplaced by a quantity δX and δY. We will describe the effect of each mirror by a matrix of two dimensions.

M_5 does not make a rotation of the image, only increases or decreases the error along the same axis by a factor m_5. M_3 rotates the plane as a function of elevation. Finally, an error in X and Y in M_2 is converted to a collimation error in azimuth and an offset in elevation respectively which depends on the equivalent focal length of the telescope:

$$\begin{pmatrix} \delta Az \\ \delta El \end{pmatrix} = \begin{pmatrix} K/\cos el & 0 \\ 0 & K \end{pmatrix} \begin{pmatrix} \cos el & -\sin el \\ \sin el & +\cos el \end{pmatrix} \begin{pmatrix} m_5 & \\ 0 & m_5 \end{pmatrix} \begin{pmatrix} \delta X \\ \delta Y \end{pmatrix}$$

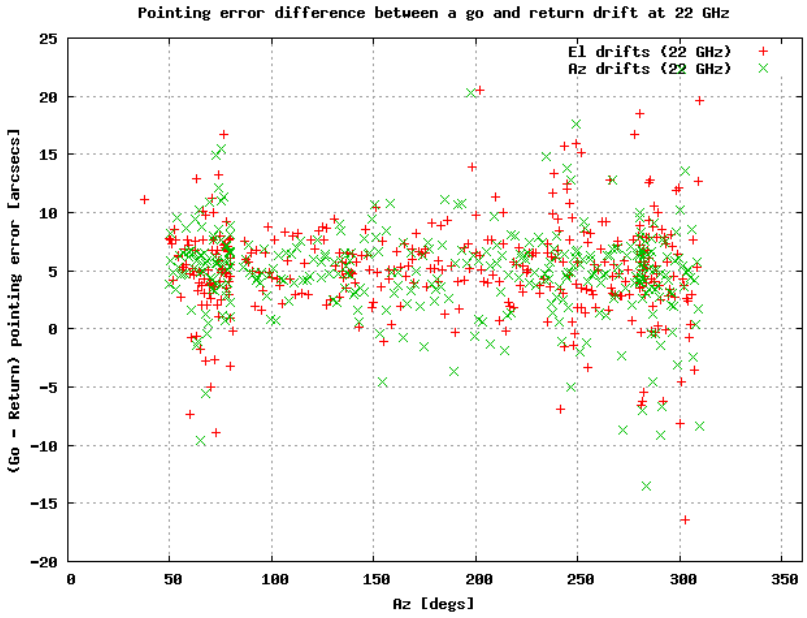

Figure 3: *Pointing error difference between two subscans along the same direction (azimuth or elevation) but opposite sense at 22 GHz. Scans were 600 arcsecs long and had a spatial resolution of 10 arcsecs per point. First subscan is always in increasing order along that axis. The result is obtained by substracting the second subscan to the first one.*

where $K = 1/f_{eq}$. The 40 m radiotelescope has an equivalent focal length of 316.6 m and hence $K(arcsecs/mm) = 3.16\ 10^{-6}\, 2.06\, 10^5 = 0.6$. Multiplying the matrixes we get:

$$\delta Az = m_5 K \delta X - m_5 K \tan el\, \delta Y \quad (1)$$

$$\delta El = m_5 K \sin el\, \delta X + m_5 K \cos el\, \delta Y \quad (2)$$

which could be written as:

$$\delta Az = P_1^{m5} + P_3^{m5} \tan el \quad (3)$$

$$\delta El = P_8^{m5} \sin el + P_9^{m5} \cos el \quad (4)$$

where the superscript "m5" stands for Nasmyth mirror 5, and means that these coefficients come from a horn missalingment after mirror M_5. Since pointing errors from CLASS are collimation errors we should use the following formulae:

$$\delta Az^c = m_5 K \cos el\, \delta X - m_5 K \sin el\, \delta Y \quad (5)$$

$$\delta El = m_5 K \sin el\, \delta X + m_5 K \cos el \delta Y \quad (6)$$

where δAz^c is the pointing error for azimuth drifts in CLASS. δX increases when we move the horn towards the "right" as we see the vertex of the antenna from the horn. δY increases when we move the horn away from the ground. Pointing errors are proportional to the shift of the horn and to the magnification of the antenna and depend on the elevation.

The previous scenario is approximately the one at the 40 m radiotelescope. In the case of the X receiver, behind M3 and M4 (a flat mirror), there is an offset parabola (M5) and a dichroic hiperbolic mirror. At C band the dichroic hiperbolic mirror is removed. At 22 GHz radiation goes straight from M4 across a hole in M5 and is reflected in a another hiperbolic mirror before entering the horn. This means that in all cases the equivalent focal distance is modified (shortened) using spherical mirrors and hence computing the correspondance between a physical displacement and an angular error is not straightforward.

5 Data reduction

Data were written in CLASS format by the control system (de Vicente 2010c). The drifts were reduced using CLASS (version aug08a) in continuum mode and written in ASCII files with azimuth, elevation, drift type (azimuth or elevation) and the result of the fit per subscan. This version of CLASS allows to produce two formats: the FIT format and the POINT format. None of them is completely useful for us since the first one contains the CLASS subscan identification, azimuth and elevation at which the observation was done and the fit result, and the second, the scan identification, the CLASS subscan identification, type of pointing drift (wether it is an azimuth or an elevation drift), azimuth and elevation at which the subscan was done and the result of the fit result except the pointing error which is replaced by a collimation error with a buggy behaviour.

To solve this issue the author wrote a simple python script which combines both files into one. The final file contains 14 columns: two scan identifiers, type of drift, azimuth, elevation, gaussian fit parameters with their errors, and the name of the source. This file is read by the pointing reduction Java software written by Alonso et al. (2010). This application makes a fit to the observations and displays the computed parameters and the results from the fit on top of the data in a graph. Observations with erroneous results are edited within the application or previously with an editor. This report shows several figures produced by this application with results from the pointing model fit.

Below we include the python script used to combine both file formats:

```
import sys, string, os

def main(args):

        fileIn1 = args[1]
        fileIn2 = args[2]
        fileOut = args[3]

        try:
                fIn1 = open(fileIn1,'r')
                fIn2 = open(fileIn2,'r')
        except:
                print "\nImposible abrir archivos de entrada %s %s" % (fileIn1, fileIn2)
                sys.exit(-1)

        try:
                fo = open(fileOut,'w')
        except:
                print "\nImposible abrir el archivo de salida %s %s" % (fileOut)
                sys.exit(-1)
```

```
        line1 = fIn1.readline()
        line2 = fIn2.readline()

        while line1 != "" and line2 != "":
            #print line1, line2
            if line1[0] != '!' and line2[0] != '!':
                 if "/" in line1 or "/" in line2:
                        pass
                 else:
                        listLine1 = line1.split()
                        listLine2 = line2.split()
                 #     1159 19517   1    63.911    15.468    11.055  -3861.43     0.68  0   0    394.23     1.
                 #     2890   62.1       34.9      0.120E+04  4.12        49.6     0.432        293.      1.06
                        print listLine1
                        print listLine2
                        scanN = int(listLine1[0])
                        gildasScan1 = int(listLine1[0])
                        gildasScan2 = int(listLine2[0])
                        if listLine1[2] == '1':
                             drift = "Az"
                        else:
                             drift = "El"
                        if gildasScan1 == gildasScan2:
                             lineOut = "%s   %s   %s   %s   %s   %s   %s   %s   %s   %s   %s   %s   %s   %s   %s
        (listLine1[0], listLine1[1], listLine1[2], listLine1 [3], listLine1[4], \\
listLine1[5], listLine2[5], listLine2[6], listLine1[8], listLine1[9], listLine1[10], \\
listLine1[11], listLine1[12], listLine1[13], listLine1[14])
                             fo.write(lineOut)
            line1 = fIn1.readline()
            line2 = fIn2.readline()


        fIn1.close()
        fIn2.close()
        fo.close()

if __name__=='__main__':
        main(sys.argv)
```

6 Pointing at 6 GHz

The determination of the new pointing model was first done at 6 GHz. The following sources were observed for 4 days in march 2010: J0319+415 (3C84), J0437+296 (3C123), J2253+161 (3C274) and J0423-013. The sky coverage was not complete due to time restrictions and occupaince of the telescope, but we found it acceptable. Sources were chosen based on their brightness and distribution on the sky.

Double pointing drifts were $2400''$ long and lasted for 60 seconds. This provides a spatial resolution of $40''$ per point, which is roughly 14% of the HPBW. Double pointing drifts may generate a pointing difference of $40''$ between a drift in one direction and the opposite.

Figures 4 and 5 display the azimuth and elevation errors as a function of azimuth and elevation and the predicted errors for the computed pointing parameters. After determining the new pointing parameters, they were included in the antenna pointing model and the pointing session was repeated again. Parameters and the rms of the fit before the model and after applying it are summarized in Table 1. Errors from the second iteration are displayed in Figures 6 and 7.

The parameter residual ($< \sigma(P) >$) is defined as the mean (geometric) variance of each parameter. The mean deviation ($\sigma(dev)$) is the rms of the difference between the data and the

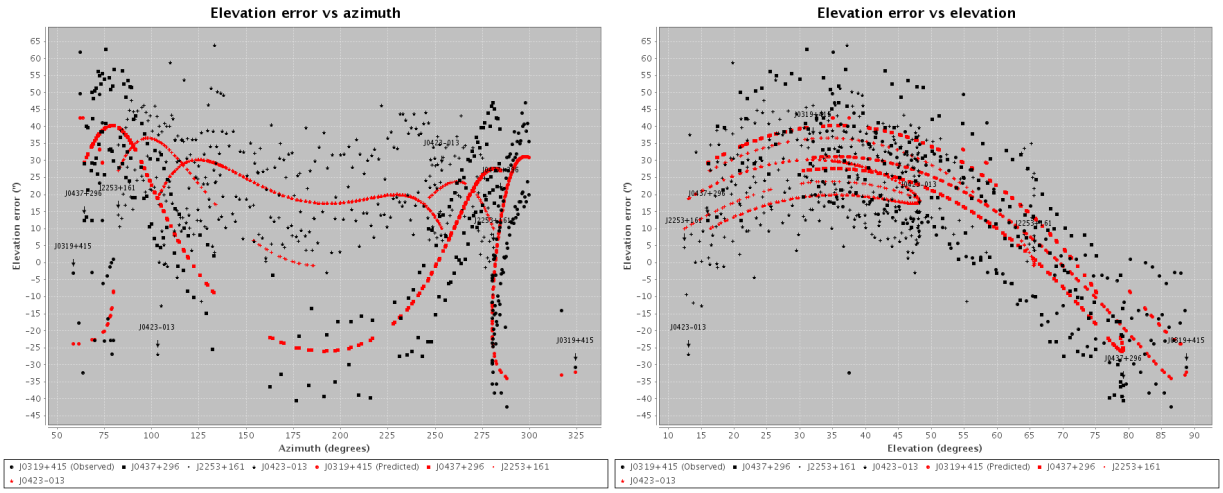

Figure 4: *Left: Elevation error versus azimuth at 6 GHz. Right: Elevation error versus elevation at 6 GHz.*

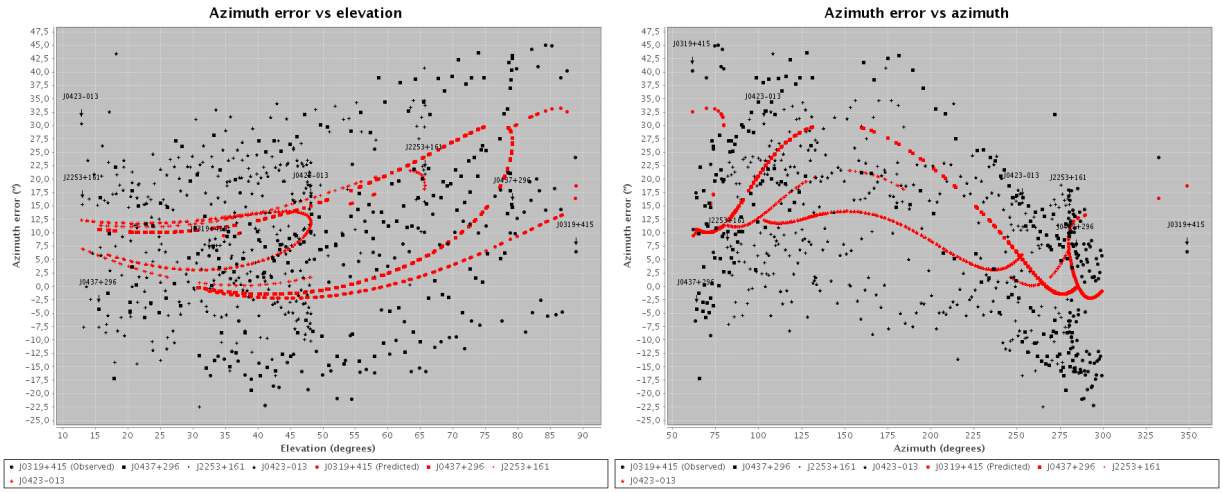

Figure 5: *Left: Azimuth error versus elevation at 6 GHz. Right: Azimuth error versus azimuth at 6 GHz.*

model computed from whole set of data.

7 Pointing at 22 GHz

Pointing at 22 GHz was done on a set of 5 sources: J0319+415 (3C84), J1230+123 (3C274), J2253+161 (3C454.3), J0437+296 (3C123) and Jupiter. The starting pointing model was model (1) at 6 GHz. Sky coverage was a bit incomplete. The second block of observations was per-

Parameter	Model (0)	Δ P (1)	Model (1)	Δ P (2)	Model (2)
P_1 ($''$)	2570	-42	2528	3	2531
P_2 ($''$)	54	58	112	-7	105
P_3 ($''$)	0	-30	-30	6	24
P_4 ($''$)	0	6	6	-3	3
P_5 ($''$)	0	11	11	-9	2
P_7 ($''$)	-915	-154	-1068	4	-1064
P_8 ($''$)	0	114	114	-8	106
P_9 ($''$)	465	147	578	38	616
$< \sigma(P) >$ ($''$)		12		12	
σ(dev) ($''$)		12		12	

Table 1: *C band pointing model. Model(0) is the starting pointing model. Model (1) is the result from the first iteration, Model (2) the result from the second iteration. Units are arcsecs*

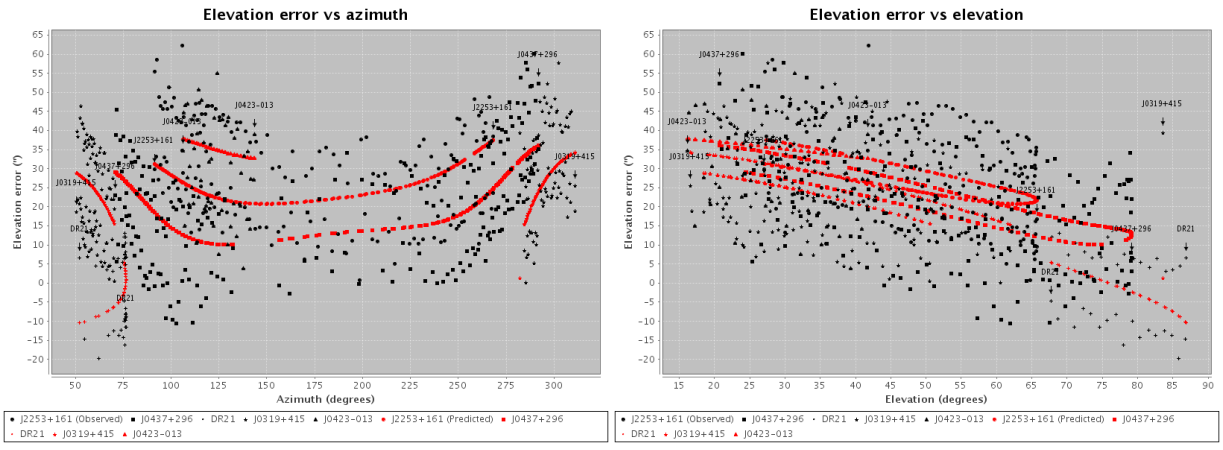

Figure 6: *Left: Elevation error versus azimuth at 6 GHz. Right: Elevation error versus elevation. Second (final) iteration.*

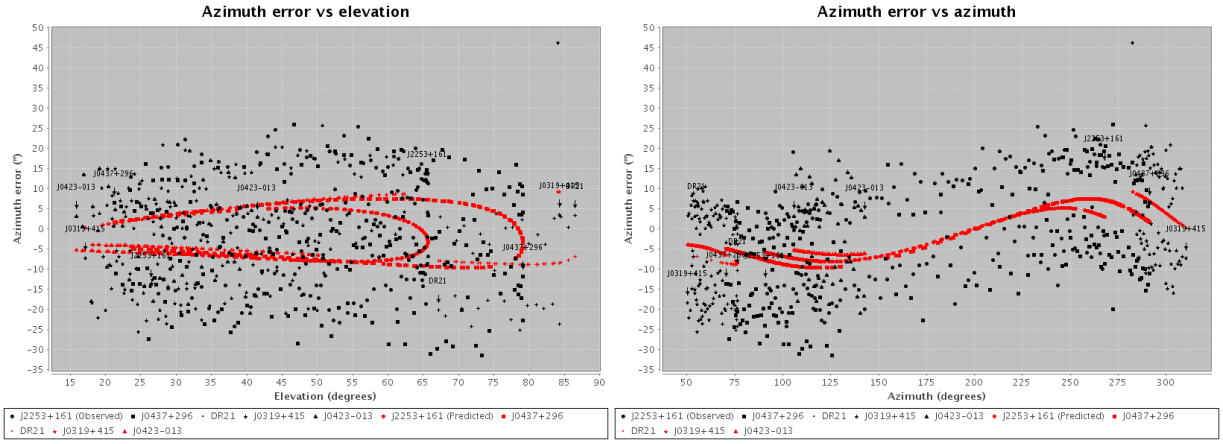

Figure 7: *Left: Azimuth error versus elevation at 6 GHz. Right: Azimuth error versus azimuth at 6 GHz. Second (final) iteration.*

formed after correcting the pointing model from session 1. Sources observed were: J1229+020 (3C273), J1230+123 (3C274), J0437+296 (3C123), DR21, and Jupiter. Each scan was composed of 4 subscans 600 arcsecs long that lasted 60 seconds and the spatial resolution was 10 arcsecs (14% of the HPBW). Two subscans were in azimuth and two in elevation. Results from both iterations are shown in table 2. All parameters were set free.

Inspection of Figs. 8 and 9, shows that elevation and azimuth error versus azimuth show a systematic effect which the pointing model cannot correct. These data were obtained using the first strategy described in section 2. Further pointing sessions should be performed using stategy 2 and once the surface is adjusted after holography measurements. Severeal positions of the 22 GHz horn will be tested.

Parameter	Model (0)	Δ P (1)	Model (1)	Δ P (2)	Model (2)
P_1 ($''$)	2528	12	2540	1	2541
P_2 ($''$)	112	-24	88	4	92
P_3 ($''$)	-30	24	-6	-6	-12
P_4 ($''$)	6	-1	5	-1	4
P_5 ($''$)	11	-4	7	1	8
P_7 ($''$)	-1068	-20	-1088	6	-1082
P_8 ($''$)	114	0	114	-10	104
P_9 ($''$)	612	4	616	-6	610
$< \sigma(P) >$ ($''$)		7		7	
σ(dev) ($''$)		18		9	

Table 2: *22 GHz band pointing model. Model(0) is the starting pointing model. Model (1) is the result from the first iteration, Model (2) the result from the second iteration. Units are arcsecs*

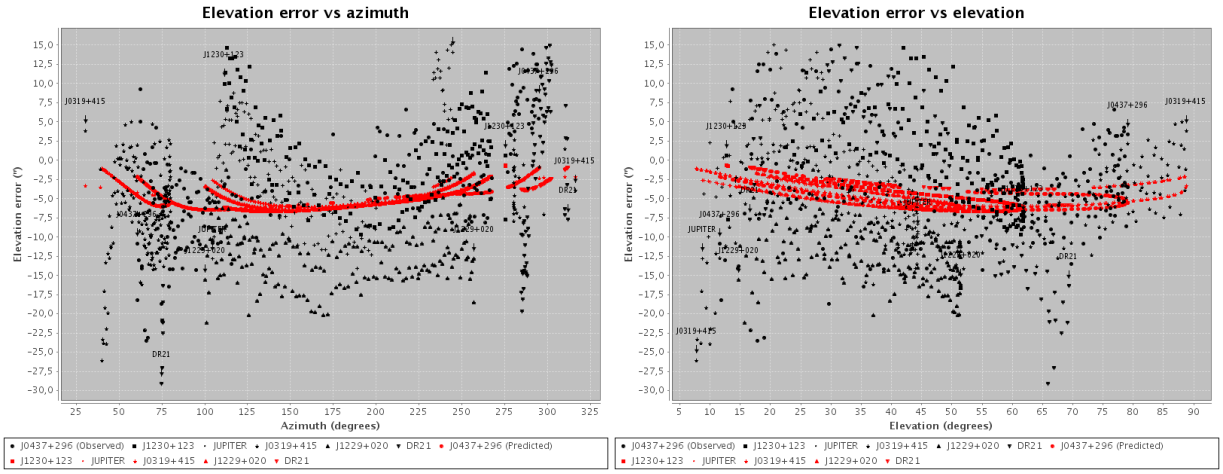

Figure 8: *Left: Elevation error versus azimuth at 22 GHz. Right: Elevation error versus elevation at 22 GHz. Second (final) iteration.*

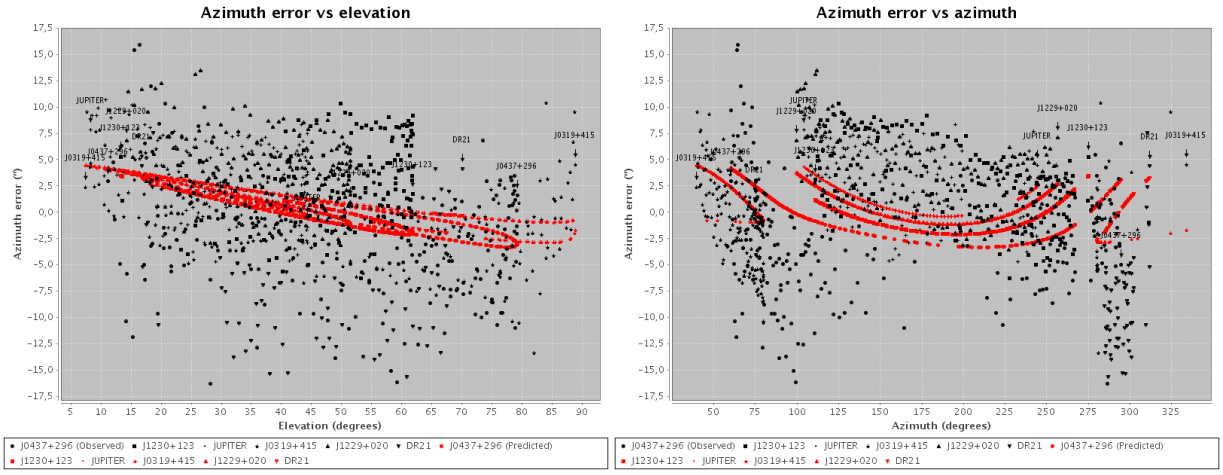

Figure 9: *Left: Azimuth error versus elevation at 22 GHz. Right: Azimuth error versus azimuth at 22 GHz. Second (final) iteration.*

8 Pointing at 8 GHz

While this report was been written, we discovered that the X band horn was incorrectly placed. The X band cryostat may house two horns: an X band horn and a Q band horn (not installed yet by this time) and they should be separated by a distance of 170 mm. However the real distance is 150 mm. As a consequence the horn is shifted at least 10 mm from its optimum position along a line parallel to the elevation axis. Two more errors may be present. The support table where the cryostat is attached may also have an error along that same axis which ammounts up to 5 mm, but its sense is unknown and it may decrease or increase the previous error. Finally a third error is present: the horn is tilted in elevation from its optical axis.

The horizontal error is visible by looking at the dichroic mirror and the X band horn from M4 and using the supporting screws, the dichoric mirror and the parabolic mirror after M4 as a reference for the eye. In order to test this missalignment we made several measurements at three different positions of the X horn to find its optimum position. The one with the maximum gain should be used.

There is a second effect that may impact pointing. It is caused by a faulty brake in the motor that raises and lowers the dichroic mirror. Its nominal position, when observing at X band, is 703 mm. We have observed that, in some cases, the dichroic mirror falls along its support mast several millimeters or even centimeters. To avoid that this effect confused our measurements, we checked that, during the pointing sessions, the mirror did not move from its nominal position.

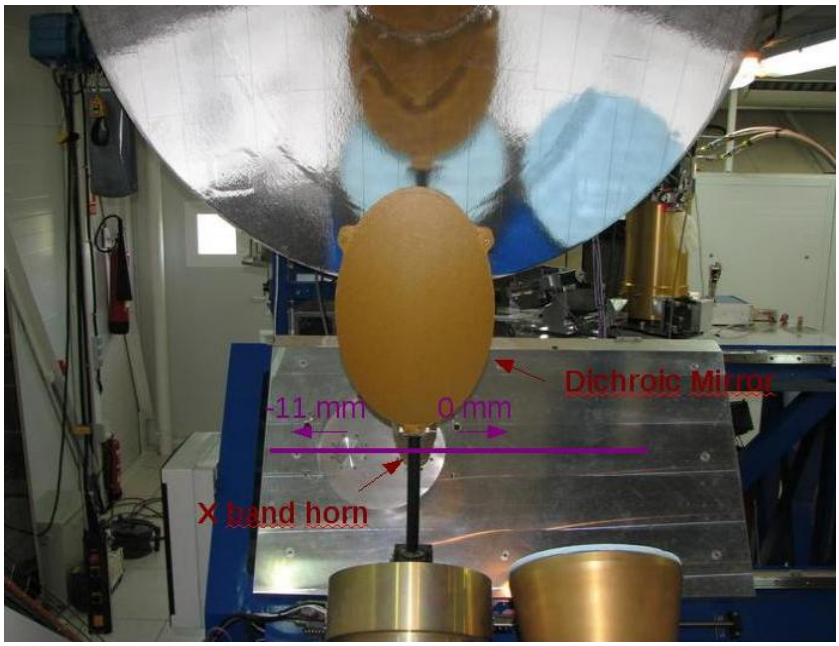

Figure 10: *X band horn, dichoric mirror and parabolic mirror. The table that supports the cryostat can be moved along the X axis (magenta line). The shown position is -5.5 mm. Positions 0 and -11 mm are also shown in the image. The dichroic mirror is in its highest position and may be shifted along its mast. The picture is taken from M4, that is, where radiation comes from.*

Pointing at 8 GHz was done on the following sources: J039+415, J1230+123, J0437+296, J1229+020 and J0423-013. The starting pointing model was the final pointing model for 22 GHz. Each scan was composed of 4 subscans 600 arcsecs long that lasted 60 seconds and the spatial resolution was 27 arcsecs (11% of the HPBW). Two subscans were in azimuth and two in elevation. Results from both iterations are shown in Table 3.

Parameter	Model (0)	Δ P (1)	Model (1)	Δ P (2)	Model (2)
P_1 ($''$)	2541	-2	2539	1	2540
P_2 ($''$)	92	-12	80	6	86
P_3 ($''$)	-12	-2	-14	30	16
P_4 ($''$)	4	4	8	-3	5
P_5 ($''$)	8	2	10	-4	6
P_7 ($''$)	-1082	-43	-1125	5	-1120
P_8 ($''$)	104	12	116	-2	114
P_9 ($''$)	610	-12	598	2	600
$< \sigma(P) >$ ($''$)		12		11	
σ(dev) ($''$)		30		30	

Table 3: *X band pointing model. Model(0) is the starting pointing model. Model (1) is the result from the first iteration (horn at 0.0 mm) and model (2) the result from the second iteration (horn at 0.0 mm) . Units are arcsecs*

Parameter	Original val.	$\delta X = 0.0$ mm	$\delta X = -5.5$ mm	$\delta X = -10.5$ mm
P_1 ($''$)	2539	-16	-17	-14
P_2 ($''$)	80	29	30	30
P_3 ($''$)	14	9	10	8
P_4 ($''$)	8	-3	-2	-2
P_5 ($''$)	10	-8	-5	-6
P_7 ($''$)	-1120	194	118	155
P_8 ($''$)	116	-164	-93	-127
P_9 ($''$)	598	-90	-57	-74
$< \sigma(P) >$ ($''$)		12	12	12
σ(dev) ($''$)		30	30	30

Table 4: *X band pointing model for 3 focus cases in which there is a lateral horn shift of 0.0 mm, -5.5 mm and -10.5 mm. Negative values imply that the horn moves away from the elevation axis. The horn values values are relative to the nominal position. The used parameter values are in the first column. Columns 2, 3 and 4 contain corrections to be applied to values in the first column.*

Several pointing drifts were performed moving the X band horn to check the pointing effects of such displacements and the gain drop associated to them. The X band horn was shifted along a line parallel to the elevation axis (and hence to the ground) by a total ammount of 20 mm. The first series of measurements were done towards 3C274 at an elevation range between 18 and

20 degrees elevation approximately with the horn in positions 10.0 mm, 0.0 mm, -5.5 mm and -10.5 mm. The second series was performed at an elevation range between 74 and 80 degrees towards 4C39.25 (a source three times weaker than the previous one). The data for each source were obtained in a time span of 40 minutes.

According to equations 5 and 6 the expected pointing errors, if the horn is moved only along the X axis, should be:

$$\delta Az^c = -m_5 \cos el\, \delta X \quad (7)$$

$$\delta El = -m_5 \sin el\, \delta X \quad (8)$$

because a positive shift according to the table where the horn is mounted, is a movement to the left (see Fig. 10). Table 5 summarizes the results. As we can see there, the data match the previous formulae. The proportionality constant is approximately $1''$/mm. The gain drop is about 28% at high elevations and 6% at low elevations. The maximum gain is attained at $\delta X = -5.0$ mm at low elevations and at $\delta X = -10.5$ mm at high elevations. This difference is consistent with the observed gain drop at X band at different elevations discussed in de Vicente (2010b). The fact that the best X position differs at low and high elevations may point to a tilt in the subreflector. This tilt may cause that the focus of radiation traces a quarter of a circle in the focal plane as the antenna moves from low elevations to high elevations, shifting the optimum position of the horn.

δX (mm)	T_a (k)	$\delta Az^c('')$	$\delta El('')$	El (°)
10.0	11.3± 0.3	11.5	21	19
0.0	12.0± 0.3	23	28	18
-5.5	12.0± 0.3	26	20	19
-10.5	11.8± 0.3	30	20	20
10.0	2.6± 0.3	20	-18	78
0.0	3.1± 0.3	21	-7.5	74
-5.5	3.5± 0.3	18	5.5	77
-10.5	3.6± 0.3	17.5	5.0	79

Table 5: *Results from pointing drifts with X horn at different positions and at two elevations. The horn position is relative to the nominal positions. Maximum antenna temperature is at -5.5 mm at 20 degrees elevation and -10.5 mm at 75 degrees elevation.*

As a conclusion from the latter measurements, the X band horn will be located at -5.5 mm and the pointing model will be modified accordingly as summarized in Table 6. Results from the fit are in Figs. 11 and 12.

Further observations will be performed in the future to check if the subreflector is really tilted and, if so, how it affects the pointing and the best X band horn position.

Parameter	Model
P_1 ($''$)	2522
P_2 ($''$)	110
P_3 ($''$)	-4
P_4 ($''$)	6
P_5 ($''$)	5
P_7 ($''$)	-1007
P_8 ($''$)	23
P_9 ($''$)	541
$< \sigma(P) >$ ($''$)	12
σ(dev) ($''$)	30

Table 6: *Final X band pointing model with the horn at -5.5 mm, obtained from a pointing session with 6 radiosources.*

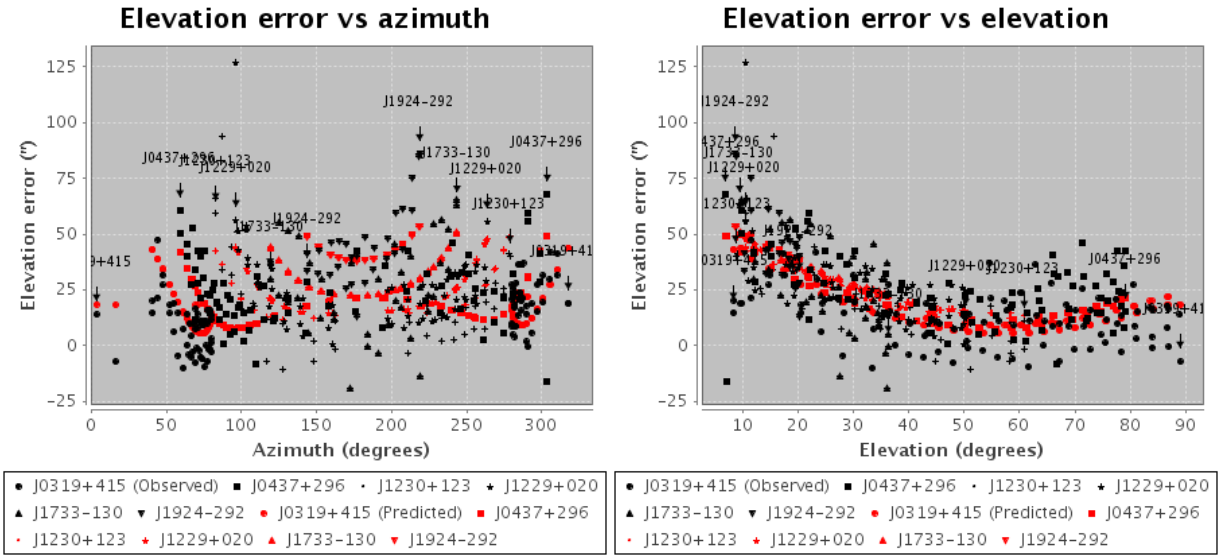

Figure 11: *Left: Elevation error versus azimuth at 8 GHz. Right: Elevation error versus elevation at 8 GHz. Horn in -5.5 mm.*

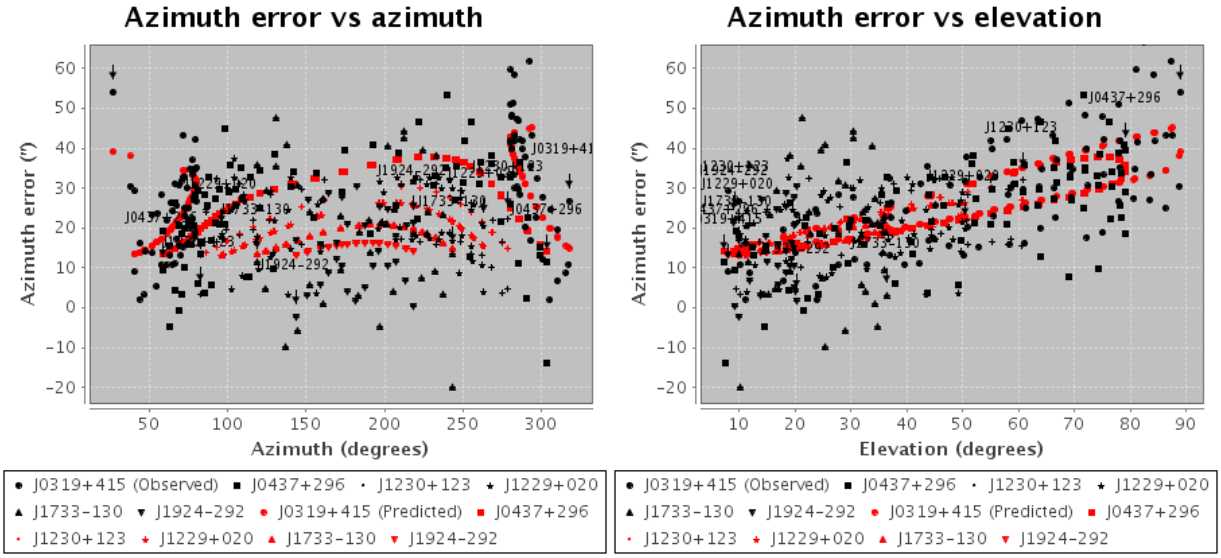

Figure 12: *Left: Azimuth error versus azimuth at 8 GHz. Right: Azimuth error versus elevation at 8 GHz. Horn in -5.5 mm.*

9 The tilt of the elevation axis

The tilt of the azimuth axis of the antenna has a pointing effect on elevation and on azimuth via parameters P_4 and P_5 as follows:

$$\begin{aligned} \Delta El &= P_4 \sin Az + P_5 \cos Az \\ \Delta Az &= -P_4 \cos Az \tan El + P_5 \sin Az \tan El \end{aligned}$$

where P_4 is the tilt angle towards the West and P_5 towards the South, ΔEl and ΔAz are the elevation and azimuth errors and Az and El are the observed azimuth and elevation.

Fig. 13 depicts the elevation error predicted from the pointing models at 6, 8 and 22 GHz. The tilt direction is a function of the ratio between P_4 and P_5 and its relative signs and it is easily determined from the figure: the direction of tilt is where the elevation error is highest with a negative sign. The magnitude of the tilt is given by the amplitude of the resulting curve at its maximum elevation error. According to this criterium the antenna is tilted $9''$ towards $\sim 230 \pm 14$ degs. That is towards the South-West.

This behaviour can be confirmed using both inclinometers installed in the 40 m antenna close and above the elevation encoders (Fig 14). Each inclinometer can be thought of as composed of a pendulum which measures the angle with a line perpendicular to the floor in two dimensions: X and Y. The Y axis is parallel to the elevation axis and the X axis is a horizontal line perpendicular to Y axis. For the time being its sense is unknown. The reference system moves with the inclinometer.

In order to get the azimuth axis tilt, the antenna is turned at a constant velocity around the azimuth axis. The results are shown in Fig. 15. The curves have been shifted along the Y

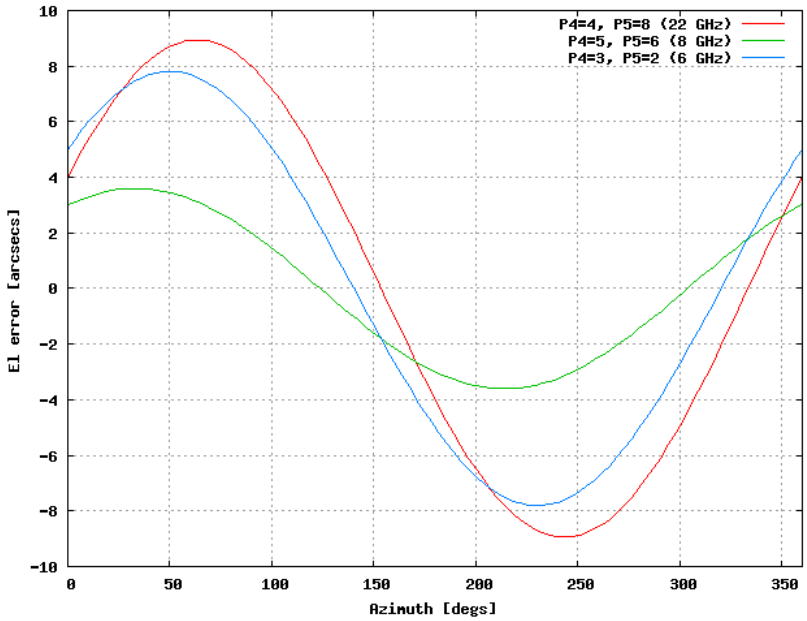

Figure 13: *Elevation error versus azimuth at 6, 8 and 22 GHz. The minimum happens towards the direction of the tilt ($\simeq$ 230 degs). North is towards 0 degrees azimuth and East towards 90 degrees.*

Figure 14: *Inclinometer (white box) above encoder 1 (black cylinder). This is the left side as seen from the receiver cabin.*

axis so that the original position, before the antenna starts moving, read zero. This operation is basically finding the offset and correcting it.

It is expected that when the antenna starts turning, Y positions from both inclinometers readouts increase (due to centrifugal force). The tilt should be visible on top of that plateau. The theoretical expected curve from the inclinometers is a sinusoid. Results from the X axis and Y axis in each inclinometer should be similar but shifted 90 degrees in azimuth, since after a rotation of 90 degrees in azimuth, X and Y axis are interchanged with respect to a fixed reference frame. Results from inclinometer 1 and 2 should also be the same but shifted 180 degrees. This is obvious since X axis at the left has an opposite sense to the axis at the right referred to a fixed reference frame. The same happens for Y axis.

According to Fig. 15, Y axis show a maximum and a minimum where both curves differ most: $\sim 170^\circ$ and $\sim 340^\circ$. The maximum and minimum for the X axis happen at $\sim 260^\circ$ and $\sim 70^\circ$. As expected, the Y and X minimum and maximum pairs differ $\sim 180^\circ$ and the values between the X and Y inclinometers differ $\sim 90^\circ$ degrees. The azimuth axis should be then tilted either at an azimuth of $\sim 260^\circ$ or at $\sim 70^\circ$. To find out which is the sense of the X axis we can observe that when the antenna accelerates to reach a stable speed, the X readout suffers a jump, due to inertia. The antenna started moving from -50° to positive values, and the readouts from X axis in both cases decreased suddenly. That means that X axis at inclinometer in the right points towards the south when the antenna is at 0°. That is equivalent to saying that it points in the sense of the rotation, when rotation is clockwise. If inclinometer 2 is at the right, while looking at the vertex from the receiver cabin, then the antenna is tilted towards azimuth $\sim 260^\circ$. This value approximately matches that from the pointing model.

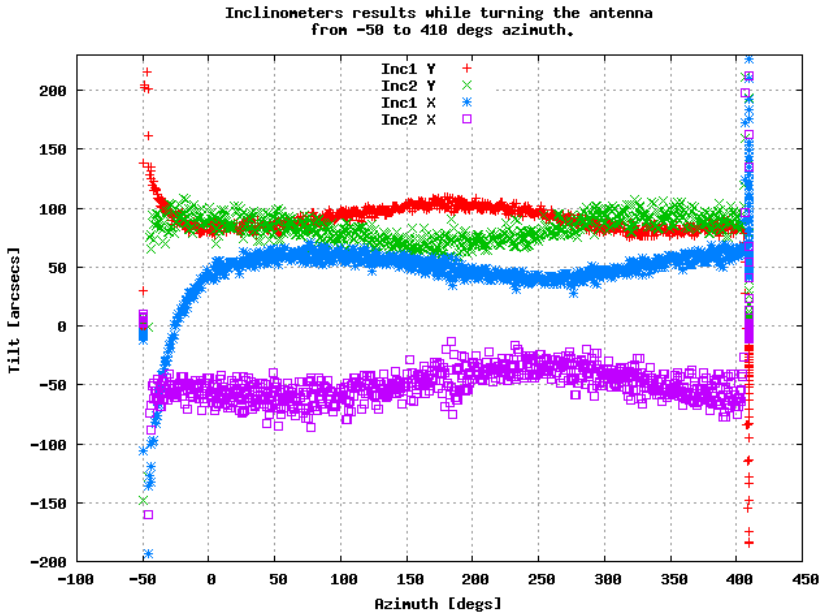

Figure 15: *Inclinometers results.*

The ammount of the tilt is approximately the amplitude of each sinosuid. Averaging the

four curves we get:

$$Amp = \frac{29 + 18 + 27 + 23}{2\,4} = 12'' \pm 2'' \tag{9}$$

Conclusion: According to the pointing model the azimuth axis is tilted $9''$ towards azimuth 230°, while according to the inclinometers it is tilted $12''$ towards azimuth 260°.

10 Final results

Table 7 summarizes the pointing models for the three frequencies. The pointing model for X band is the one obtained with the horn in position -5.5 mm. Models are roughly similar, being the most different the X band one. Differences are significative in P_7, P_8 and P_9.

Parameter	6 GHz	8 GHz	22 GHz
P_1 ($''$)	2531	2522	2541
P_2 ($''$)	105	110	92
P_3 ($''$)	-24	-4	-12
P_4 ($''$)	3	6	4
P_5 ($''$)	2	5	8
P_7 ($''$)	-1064	-1007	-1082
P_8 ($''$)	106	23	104
P_9 ($''$)	616	541	610

Table 7: *Current pointing models at the 40 m radiotelescope. X band*

The difference in parameters P_8 and P_9 are easily understandable as arising from horn offsets in X and Y. However a difference in P_7 cannot be explained from an error after the Nasmyth mirror M3. We have tried to fix P_7 to a nominal vaue and fit the rest of parameters but this causes a clear wrong fit. We should investigate further why P_7 at X band differs from the pointing results at 6 and 22 GHz.

New pointing models should be derived if we find that the best position of the X band and 22 GHz horns differ from the current ones.

References

[Alonso et al. 2010] T. Alonso, P. de Vicente, V. Bujarrabal. "Implementation of the pointing model for the 40m OAN radiotelescope". Informe Técnico OAN 2010-3. 2010

[de Vicente & Barcia 2007] P. de Vicente, A. Barcia. "Deconstructing a pointing model". Informe Técnico OAN-2008-27. 2007

[de Vicente 2008a] P. de Vicente. "Checking the pointing corrections implementation for the 40m radiotelescope". Informe Técnico OAN-2008-7. 2008

[de Vicente 2008b] P. de Vicente. ”Preliminary characterization of the 40m radiotelescope at 22 GHz”. Informe Técnico OAN-2008-8. 2008

[de Vicente 2010a] P. de Vicente, K. Matull, E. Sust, C. Albo. ”Encoder hysteresis at the 40m radiotelescope” Informe Técnico OAN-2010-2. 2010

[de Vicente 2010b] P. de Vicente. ”Characterization of the 40m radiotelescope at 5, 6, 8 and 22 GHz”. Informe Técnico OAN-2010-10. 2010

[de Vicente 2010c] P. de Vicente. ”Data acquisition and preliminary processing at the 40 m telescope”. In preparation